Accepted Manuscript

Modelling, kinematic parameter identification and sensitivity analysis of a Laser Tracker having the beam source in the rotating head

J. Conte, J. Santolaria, A.C. Majarena, R. Acero

PII: S0263-2241(16)30037-9
DOI: http://dx.doi.org/10.1016/j.measurement.2016.03.059
Reference: MEASUR 3917

To appear in: *Measurement*

Received Date: 22 October 2014
Revised Date: 18 July 2015
Accepted Date: 26 March 2016

Please cite this article as: J. Conte, J. Santolaria, A.C. Majarena, R. Acero, Modelling, kinematic parameter identification and sensitivity analysis of a Laser Tracker having the beam source in the rotating head, *Measurement* (2016), doi: http://dx.doi.org/10.1016/j.measurement.2016.03.059

Modelling, kinematic parameter identification and sensitivity analysis of a Laser Tracker having the beam source in the rotating head

J. Conte[1], J. Santolaria[1], A.C. Majarena*[1], R. Acero[2]

[1]Department of Design and Manufacturing Engineering, Universidad de Zaragoza, Zaragoza, Spain

[2]Centro Universitario de la Defensa, Zaragoza, Spain

*Corresponding author: majarena@unizar.es, Tel. 34876555453.

Abstract

This paper presents a new kinematic model, a parameter identification procedure and a sensitivity analysis of a laser tracker having the beam source in the rotating head. This model obtains the kinematic parameters by the coordinate transformation between successive reference systems following the Denavit-Hartenberg method. One of the disadvantages of laser tracker systems is that the end-user cannot know when the laser tracker is working in a suitable way or when it needs an error correction. The ASME B89.4.19 Standard provides some ranging tests to evaluate the laser tracker performance but these tests take a lot of time and require specialized equipment. Another problem is that the end-user cannot apply the manufacturer's model because he cannot measure physical errors. In this paper, first the laser tracker kinematic model has been developed and validated with a generator of synthetic measurements using different meshes with synthetic reflector coordinates and known error parameters. Second, the laser tracker has been calibrated with experimental data using the measurements obtained by a coordinate measuring machine as nominal values for different strategies, increasing considerably the laser tracker accuracy. Finally, a sensitivity analysis of the length measurement system tests is presented to recommend the more suitable positions to perform the calibration procedure.

Keywords: Laser tracker, modelling, kinematic parameter identification, synthetic generator, sensitivity analysis

1. Introduction

There has been a rapid development in recent years of long-range dimensional metrology systems for the verification of large-scale pieces, such as those in the aeronautic, spatial or naval sectors. The interest in laser trackers (LTs) has been increasing because of their advantages in terms of accuracy, portability, flexibility (wide range of angles and distances in measurement), high speed in data acquisition, reliability [1, 2], automatic target tracking and high sampling rate [3]. Applications of LTs are very wide. For example, in [4], authors calibrate a robot using a LT to acquire measurements, increasing considerably the robot accuracy, and in [5], volumetric verification of machine

tools is performed using LTs. In [6], the accuracy of an arm based on parallel mechanisms is evaluated by means of a laser tracking coordinate measuring system. Other studies show the use of LTs to calibrate systems such as the calibration of a Stewart platform [7] or the calibration of an articulated arm coordinate measuring machine [8]. A LT is used in the measuring and the adjusting of the workbench for SAR antenna in [9]. An optical surface in a telescope is measured in [10], obtaining high accuracy. LT technology can also be used for monitoring structure movement [11] and in analysis of deformations of industrial elements [12]. In [13], a LT is used to calibrate a coordinate measuring machine (CMM). The method is validated using a ball plate measurement.

Although the use of this technology is increasing due to its important advantages, the mechanical assembly generates misalignments, offsets, eccentricities and non-linearities, which cause errors in the measured coordinates. LT manufactures have developed software to correct this type of errors. One of the problems that appears while measuring with a LT is that some of these errors, such as those related to angular scale errors, are considered as constants and the end-user cannot update them. LT head presents radial/tilt motion as the head spins about the vertical axis, resulting in errors in the measured range [14]. One of the disadvantages of these tracking measurement systems is that the end-user cannot know when the LT is performing a measurement properly or when it needs a new calibration. Moreover, there is no a standard calibration procedure.

The ASME B89.4.19 Standard provides some ranging tests, length measurement system tests and two-face system tests that can be performed to analyse the performance of the LT. In [15], the authors studied the relationship between geometric misalignments of these systems and performance evaluation tests recommended in the B89.4.19 standard [16], and proposed some new gauge object placement scenarios to improve sensitivity for length measurement system tests.

However, these tests do not give information about the individual error sources, and only provide information related to the suitable or unsuitable LT performance with respect to these standards. Moreover, these tests take a lot of time and require very specialized equipment. To know the individual error sources, a calibration procedure should be performed.

The kinematic model establishes mathematical relations and obtains non-linear equations that relate the joint variables with the position and orientation of the end-effector [17]. One of the most widely used kinematic methods for modelling a mechanism is the well-known Denavit-Hartenberg (D-H) method [18], which uses four parameters to model the coordinate transformation between successive reference systems [19-21]. Some studies [22, 23] present methods to obtain a complete, equivalence and proportional model to solve some limitations of this method that appear in those mechanisms with two consecutive parallel joint axes. For each revolute joint, four parameters must be considered, two linear and two rotary, applied about the non-colinear axes before and perpendicular to the translational joint axes [24].

The calibration procedure allows us to identify the kinematic parameters in order to improve the model accuracy [25], thus obtaining correction models to establish corrections in the measurement results and to quantify the effects of the influence of the variables in the final measurement.

The objective function to minimize in the identification procedure can be formulated in terms of a non-linear least-squares problem and it is usually defined as the quadratic difference of the error obtained between the measured value and the value computed for the kinematic model. The increment value established for parameters will depend on the optimization method chosen and must be defined for each iteration [26]. Numerical optimization techniques are usually used to minimize the error. The Levenberg-Marquart (L-M) [27] method presents lower computational cost, providing a solution closer to the optimum solution for the set of parameters considered, thus is one of the most widely used techniques to solve the numerical optimization algorithm.

There are few studies to calibrate a LT. In [28], the authors calibrated the azimuth angle encoder by using a rotary table torque motor to turn the platform with the LT, remaining the LT locked on to the target mirror. The LTs body moves with the platform while the LT head remains stationary. Thus, a new horizontal angle reading is compared to the rotary table encoder reading. Self-calibration methods have been used for laser tracking systems. In [29-31], this method is used to calibrate a LT by restricting retroreflector motion to an arbitrarily surface of constraints plane.

Calibration based on networks measurements consists of determining the kinematic model parameters by measuring a set of fix target locations from multiple locations of the LT. The model can be used to correct the error of the raw LT data. One of the advantages of a calibration based on network measurements is that no specialist equipment is needed. Besides, the time required to calibrate the LT decreases considerably in comparison with the time required to carry out the performance tests recommended by the ASME B89.4.19 Standard.

The aim of this work is, first, to develop a new kinematic model that allows us to perform the calibration procedure in an easy and fast way without needing specialist equipment, and second, to present a sensitivity analysis of the length measurement system tests to recommend the more suitable positions to perform the calibration procedure based on network measurements.

2. Laser Tracker Principle

A LT is a large-scale measuring instrument. This system measures relative distances, by means of a laser interferometer, and azimuth and elevation angles of a beam-steering mirror using optical encoders. The interferometer measurements are obtained relative to the starting point. Moreover, this beam must track the positions of a retro-reflector. A beam splitter mounted on a high precision universal joint deflects the beam and hits the retro-reflector. The LT beam hits the center point of the retro-reflector and is reflected

parallel by means of three perpendicularly oriented plane mirrors of the retro-reflector. When there is no relative movement between the LT head and the retro-reflector, there is no parallel displacement between the emitted and the reflected beam. However, when the retro-reflector starts moving, there is a displacement of the reflected laser beam, since, in this case, the laser beam does not hit the center point of the retro-reflector. Then the LT moves to face the retro-reflector.

The LT measures the position of the target in Spherical coordinates. The interferometer measures the distance, *d*, and the horizontal and vertical encoders provide the azimuth and elevation angles, θ and φ, respectively, as shown in Figure 1.

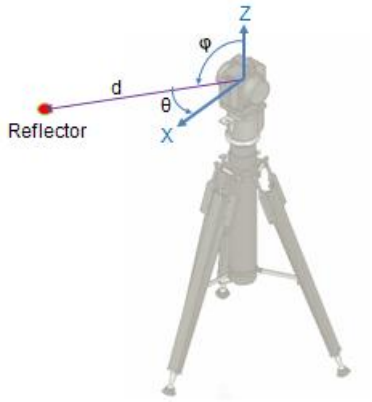

Fig.1. LT kinematics.

There are different mechanical constructions in the manufacturing of a LT. We can divide them in two main groups: LT having the laser source in the rotating head and LT having a beam steering mirror with source mounted on the standing axis. A third group of laser systems having a rotating prism mirror that steers the beam to the target can be considered.

In this work, we are going to study the first group, LT having the laser source in the rotating head, developing a new kinematic model and a calibration procedure.

3. Kinematic model

This section presents a new kinematic model that will allow us to perform the calibration procedure in an easy and fast way without needing specialist equipment.

The kinematic model of a LT can be developed by means of the D-H [18] method. This method models the coordinate transformation between successive reference systems [32], using four parameters (distances d_i, a_i, and angles θ_i, α_i). The homogenous transformation matrix between frame *i* and *i-1* depends on these four parameters as shown in Equation 1.

$$ {}^{i-1}A_i = T_{z,d} \cdot R_{z,\theta} \cdot T_{x,a} \cdot R_{x,\alpha} = \begin{bmatrix} \cos\theta_i & -\cos\alpha_i \cdot \sin\theta_i & \sin\alpha_i \cdot \sin\theta_i & a_i \cdot \cos\theta_i \\ \sin\theta_i & \cos\alpha_i \cdot \cos\theta_i & -\sin\alpha_i \cdot \cos\theta_i & a_i \cdot \sin\theta_i \\ 0 & \sin\alpha_i & \cos\alpha_i & d_i \\ 0 & 0 & 0 & 1 \end{bmatrix} \quad (1) $$

This LT can be modelled as an open kinematic chain that consists of two rotary joints and a linear joint. Figure 2 shows the reference systems used in the LT modelling.

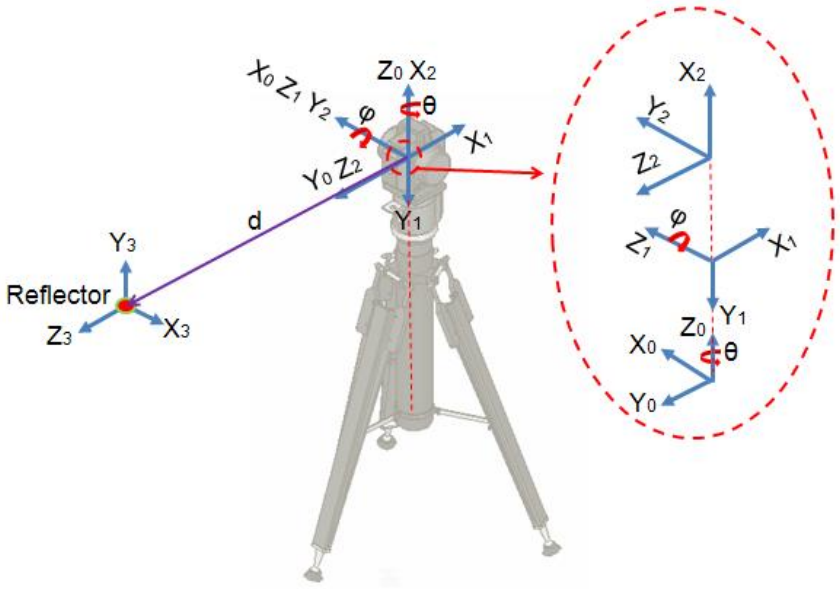

Fig 2. Reference systems used in the LT modelling.

Table 1 shows the D-H parameters of the kinematic model.

Table 1: D-H parameters.

i	α_i (º)	a_i (mm)	d_i (mm)	θ_i (º)
1	-90	0	0	θ–90
2	90	0	0	φ-90
3	0	0	d	-90

The system obtained to express the reference frame 3 (reflector location) in the reference frame 0 (origin of the LT) in terms of θ, φ and d is shown by Equations 2, 3, 4 and 5:

$$ {}^{0}T_3 = {}^{0}A_1 \cdot {}^{1}A_2 \cdot {}^{2}A_3 \quad (2) $$

$$ {}^{0}A_1 = \begin{bmatrix} \cos(\theta-90) & 0 & -\sin(\theta-90) & 0 \\ \sin(\theta-90) & 0 & \cos(\theta-90) & 0 \\ 0 & -1 & 0 & 0 \\ 0 & 0 & 0 & 1 \end{bmatrix} \quad (3) $$

$$ {}^{1}A_{2} = \begin{bmatrix} \cos(\varphi - 90) & 0 & \sin(\varphi - 90) & 0 \\ \sin(\varphi - 90) & 0 & -\cos(\varphi - 90) & 0 \\ 0 & 1 & 0 & 0 \\ 0 & 0 & 0 & 1 \end{bmatrix} \quad (4) $$

$$ {}^{2}A_{3} = \begin{bmatrix} 0 & 1 & 0 & 0 \\ -1 & 0 & 0 & 0 \\ 0 & 0 & 1 & d \\ 0 & 0 & 0 & 1 \end{bmatrix} \quad (5) $$

where θ, φ and d, are the angles and distance lectures of the angular encoders and of the linear interferometer of the LT.

Initial parameters are kept constants and the effect of their possible variations in the optimization is included by means of the error matrices.

It is not necessary to add an error parameter to consider the prove cero offset in the nominal model because the initial position coincides with the encoder reference marks. The LT has incremental encoders. Reference systems are chosen to satisfy that when the encoder of the first axis reads a value of cero, it is then aligned with axis X, and when the encoder of the second axis reads a value of cero, it is aligned with axis X_1.

The input information and the generated data will be presented in Cartesian coordinates.

The transformation from Cartesian coordinates (X, Y, Z) to Spherical coordinates (θ, φ, d) has been performed taking into account Equations from 6 to 8:

- Interferometer distance:

$$ d = \sqrt{X^2 + Y^2 + Z^2} \quad (6) $$

- Elevation angle:

$$ \varphi = a\sin\left(\frac{Z}{\sqrt{X^2 + Y^2 + Z^2}}\right) = a\sin\left(\frac{Z}{d}\right) \quad (7) $$

- Horizontal angle:

$$ \theta = a\tan 2\left(\frac{Y}{X}\right) \quad (8) $$

The elevation angle range was obtained considering the LT working range between +77º and -60º.

The transformation from Spherical coordinates (θ, φ, d) to Cartesian coordinates (X, Y, Z) is shown by Equations from 9 to 11:

$$ X = d \cdot \cos\varphi \cdot \cos\theta \quad (9) $$

$$ Y = d \cdot \cos\varphi \cdot \sin\theta \quad (10) $$

$$ Z = d \cdot \sin\varphi \quad (11) $$

The axis of rotation revolves around an axis of the reference coordinate frame with radial errors δ_x and δ_y; an axial error δ_z; and tilt errors ε_x and ε_y. These errors can be function of the rotation angle θ_z.

Errors are modelled by means of Equation 12 for rotary and linear axis [32] (see Figure 3).

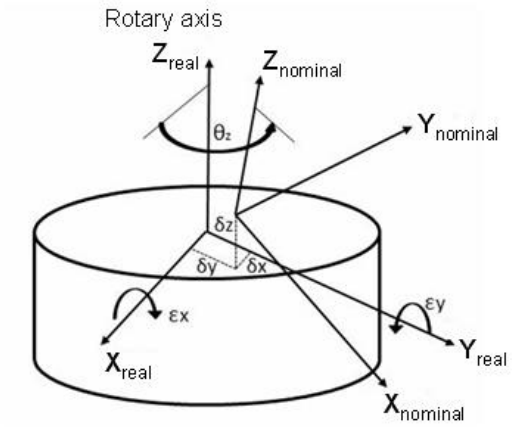

Fig 3. Errors about an axis of rotation.

$$R_{Terr} = \begin{bmatrix} \cos\varepsilon_Y \cdot \cos\theta_Z & -\cos\varepsilon_Y \cdot sin\theta_Z & sin\varepsilon_Y & \delta_X \\ \cos\varepsilon_X \cdot \sin\theta_Z + \sin\varepsilon_X \cdot sin\varepsilon_Y \cdot \cos\theta_Z & \cos\varepsilon_X \cdot \cos\theta_Z - \sin\varepsilon_X \cdot sin\varepsilon_Y \cdot sin\theta_Z & -\sin\varepsilon_X \cdot \cos\varepsilon_Y & \delta_Y \\ sin\varepsilon_X \cdot \sin\theta_Z - \cos\varepsilon_X \cdot sin\varepsilon_Y \cdot \cos\theta_Z & \sin\varepsilon_X \cdot \cos\theta_Z + \cos\varepsilon_X \cdot sin\varepsilon_Y \cdot sin\theta_Z & \cos\varepsilon_X \cdot \cos\varepsilon_Y & \delta_Z \\ 0 & 0 & 0 & 1 \end{bmatrix} \quad (12)$$

In the same way, linear axes present linear and angular errors identified with parameters δ_x, δ_y, δ_z, ε_x, ε_y and ε_z (see Figure 4).

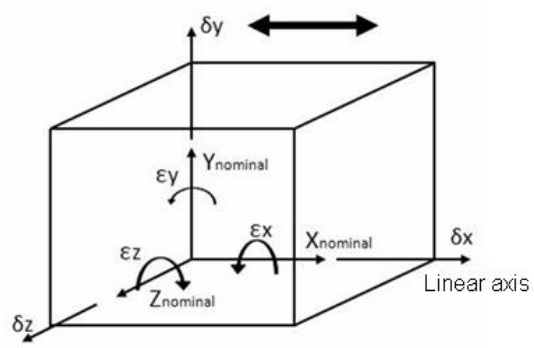

Fig. 4. Errors in a single axis linear motion.

$$T_{err} = \begin{bmatrix} 1 & -\varepsilon_Z & \varepsilon_Y & \delta_X \\ \varepsilon_Z & 1 & -\varepsilon_X & \delta_Y \\ -\varepsilon_Y & \varepsilon_X & 1 & \delta_Z \\ 0 & 0 & 0 & 1 \end{bmatrix} \quad (13)$$

The system that provides the LT model considering the error matrices is calculated introducing error matrices in Equation 2. Equation 14 gives the result:

$$ {}^{0}T_3 = {}^{0}A_1 \cdot {}^{0}\mathrm{Re}rr_1 \cdot {}^{1}A_2 \cdot {}^{1}\mathrm{Re}rr_2 \cdot {}^{2}A_3 \cdot {}^{2}T\,\mathrm{e}rr_3 \tag{14} $$

This model presents 18 error parameters given by the vector $V\varepsilon$ (Equation 15). This vector consists of the components X, Y and Z of the error parameters δ and ε for the azimuth angle, θ, elevation angle, φ, and distance, d.

$$ V_\varepsilon = [\varepsilon_{X_\theta}, \varepsilon_{Y_\theta}, \varepsilon_{Z_\theta}, \delta_{X_\theta}, \delta_{Y_\theta}, \delta_{Z_\theta}, \varepsilon_{X_\varphi}, \varepsilon_{Y_\varphi}, \varepsilon_{Z_\varphi}, \delta_{X_\varphi}, \delta_{Y_\varphi}, \delta_{Z_\varphi}, \varepsilon_{X_d}, \varepsilon_{Y_d}, \varepsilon_{Z_d}, \delta_{X_d}, \delta_{Y_d}, \delta_{Z_d}] \tag{15} $$

However, these parameters vary depending on the type of joint. These errors are function of the rotation angle in rotary joints. A model using periodic functions allows us to characterize these errors due to their periodic behaviour, as presented by Equations from 16 to 19. It can be noticed that the rotation error has both a constant component and some terms that depend on the rotation. The constant component can be considered as an offset of the encoder. The simulations performed show satisfactory results considering the second harmonic. ε_i and δ_i are error parameters for the coordinates X, Y and Z.

$$ \varepsilon_i = \varepsilon_{i1} + \varepsilon_{i2} \cdot \sin(\theta + \varepsilon_{i3}) + \varepsilon_{i4} \cdot \sin(2 \cdot \theta + \varepsilon_{i5}) \tag{16} $$

$$ \varepsilon_i = \varepsilon_{i1} + \varepsilon_{i2} \cdot \sin(\varphi + \varepsilon_{i3}) + \varepsilon_{i4} \cdot \sin(2 \cdot \varphi + \varepsilon_{i5}) \tag{17} $$

$$ \delta_i = \delta_{i1} + \delta_{i2} \cdot \sin(\theta + \delta_{i3}) + \delta_{i4} \cdot \sin(2 \cdot \theta + \delta_{i5}) \tag{18} $$

$$ \delta_i = \delta_{i1} + \delta_{i2} \cdot \sin(\varphi + \delta_{i3}) + \delta_{i4} \cdot \sin(2 \cdot \varphi + \delta_{i5}) \tag{19} $$

The function that describes the parameter behaviour in linear joints shows that these errors depend on the distance d, as shown by Equations 20 and 21. This linear axis error can be modelled considering a polynomial. The variation of this type of error is smooth in its working range, and a second order polynomial is considered sufficient to model the behaviour of this error.

$$ \varepsilon_i = \varepsilon_{i1} + \varepsilon_{i2} \cdot d + \varepsilon_{i3} \cdot d^2 \tag{20} $$

$$ \delta_i = \delta_{i1} + \delta_{i2} \cdot d + \delta_{i3} \cdot d^2 \tag{21} $$

Equations from 16 to 19 have 5 error parameters each one. Moreover, each equation is obtained for coordinates X, Y and Z, resulting in 60 error parameters. In the same way, Equations 20 and 21 are obtained for coordinates X, Y and Z, and every equation presents 3 error parameters, resulting in 18 error parameters. Thus, the kinematic model has 78 error parameters.

4. Kinematic model validation

To validate the kinematic model developed, two steps have been performed:

1) Synthetic measurements have been generated. In this step, nominal values of a mesh of reflectors and kinematic error parameters are known. Thus, we obtain the values that would measure the LT if it had the prefixed errors by means of the kinematic model developed. The objective of this phase is to generate synthetic points with a known error.
2) Using the synthetic measurements obtained in point 1) and the nominal values of the mesh, error parameters are obtained through the kinematic model. These obtained errors are compared with the prefixed errors to validate the model developed.

Next paragraphs describe these two phases.

4.1. Obtaining synthetic measurements by means of the kinematic model

A synthetic point generator consists of a set of algorithms that provide synthetic points throughout the LT workspace. This generator obtains synthetic measurements from the nominal values of a mesh of reflectors and known kinematic error parameters. The LT position and the position of the mesh with respect to the LT are also known parameters.

To perform the simulation, three mesh points have been defined.

1. A plane mesh.
   This mesh corresponds to a wall (a 2D mesh). For a constant value of *X*, *Y* varies from -10000 mm to 10000 mm with increments of 1420 mm, and *Z* varies from -1500 mm to 5500 mm with increments of 500 mm.
2. A cubic mesh
   This simulation corresponds to a mesh having constant increments of 4000 mm in the coordinates *X*, *Y* and *Z*, from -10000 mm to 10000 mm.
3. A spherical mesh
   In this case, the mesh is generated in Spherical coordinates, covering the LT range -a horizontal angle of 360º, with increments of 33º, a vertical angle from +77º to -60º with increments of 20º and a distance from 1000 mm to 15000 mm with increments of 3500 mm.

Three typical geometries of 3D mesh have been chosen to perform a parameter identification based on distance errors. Constraints are given by the mesh definition. Some authors use geometry constraints to obtain the error parameters. However, we use Euclidean distances between reflectors. These distances are independent of the mesh geometry.

Figure 5 illustrates the three mesh studied when every parameter has a value of 10 μm for linear errors and 10 μrad for rotational errors. The values introduced are close to real LT errors to better reflect a real situation while measuring with the LT.

These fix, nominal values are independent of the rotation and not present measurement noise. They are used to validate the model. Arrows represent the error with the magnification factor indicated in the figure title.

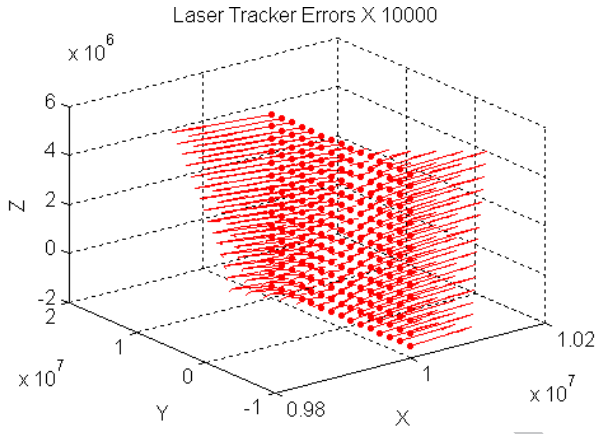

(a)

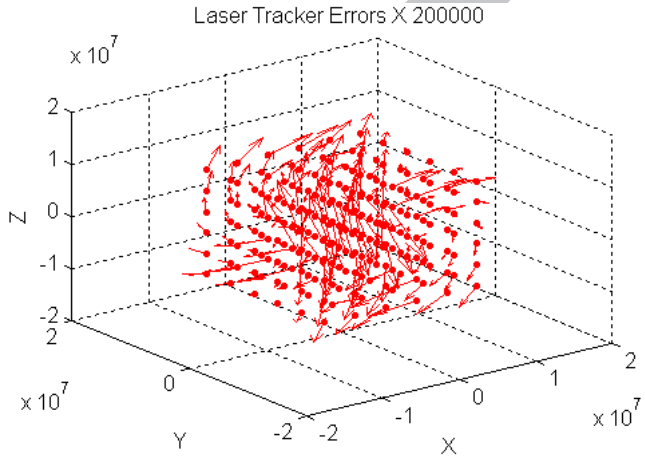

(b)

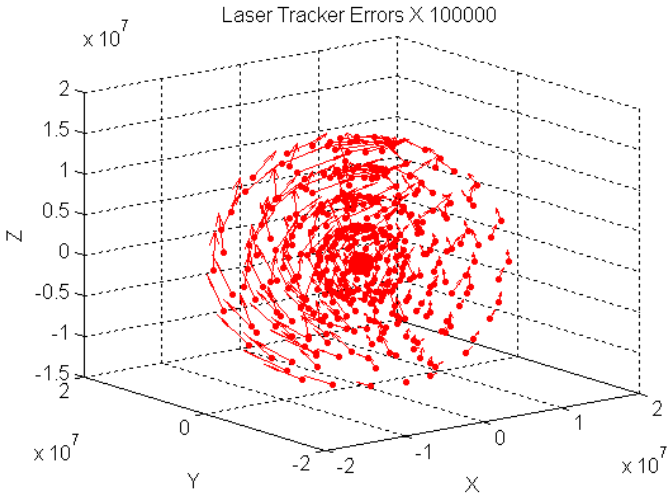

(c)

Fig 5. Meshes used in the generation of data. a) Plane mesh (2D), b) Cubic mesh (3D), c) Spherical mesh (3D).

The error matrix considers the 18 physical errors, (ε_i, δ_i), presented in section 3.1. by Equation 15, with a constant value of 10 μm for linear errors and of 10 μrad for rotary errors, as shown in Table 2.

Table 2. Error initial values used in the synthetic measurement generation.

	ε_X (μrad)	ε_Y (μrad)	ε_Z (μrad)	δ_X (μm)	δ_Y (μm)	δ_Z (μm)
θ	10	10	10	10	10	10
φ	10	10	10	10	10	10
d	10	10	10	10	10	10

This process obtains the coordinates that would measure the laser tracker if it had the errors defined from the nominal coordinates of a mesh. Thus, an optimization procedure is necessary to obtain the measured coordinates.

To do this, we defined the location of a set of reflectors with known nominal Cartesian coordinates (X_{nom}, Y_{nom}, Z_{nom}). The Spherical nominal coordinates are given by (θ_{nom}, φ_{nom}, d_{nom}). The objective is to obtain the Spherical coordinates for the reflector location that would measure a laser tracker having an error, (θ_m, φ_m, d_m). These coordinates are different from the nominal Spherical coordinates because the laser tracker has an error.

LT provides data in the LT reference system. Thus, meshes have been generated in the LT reference system.

The azimuth and elevation angles and the distance are considered the identification parameters. Thus, the Spherical nominal coordinates of the reflectors are introduced in the kinematic model as initial values. The optimization procedure varies these three parameters in every iteration defined by the sub-index *it*, (θ_{it}, φ_{it}, d_{it}), to obtain the angles and the distance that would measure the LT, (X_{it_m}, Y_{it_m}, Z_{it_m}), having an error, (ε_i, δ_i), for every point *i* of the mesh in every iteration. To obtain the mesh point coordinates affected by the LT errors, the objective function minimizes the Euclidean distance between the coordinates (X_{nom}, Y_{nom}, Z_{nom}), and (X_{it_m}, Y_{it_m}, Z_{it_m}).

Thus, Equation 22 gives the objective function introduced in the algorithm.

$$\phi = \sum_{i=1}^{n} (X_{it\_m_i} - X_{nom_i})^2 + (Y_{it\_m_i} - Y_{nom_i})^2 + (Z_{it\_m_i} - Z_{nom_i})^2 \quad (22)$$

where *n* is the number of points measured of the mesh.

The optimization obtains the Spherical coordinates (θ_m, φ_m, d_m) given by the values of (θ_{it}, φ_{it}, d_{it}) in the last iteration. These Spherical coordinates are then transformed to Cartesian coordinates obtaining the Cartesian coordinates, (X_m, Y_m, Z_m), that would measure the LT having an error. This procedure is summarized in Figure 6.

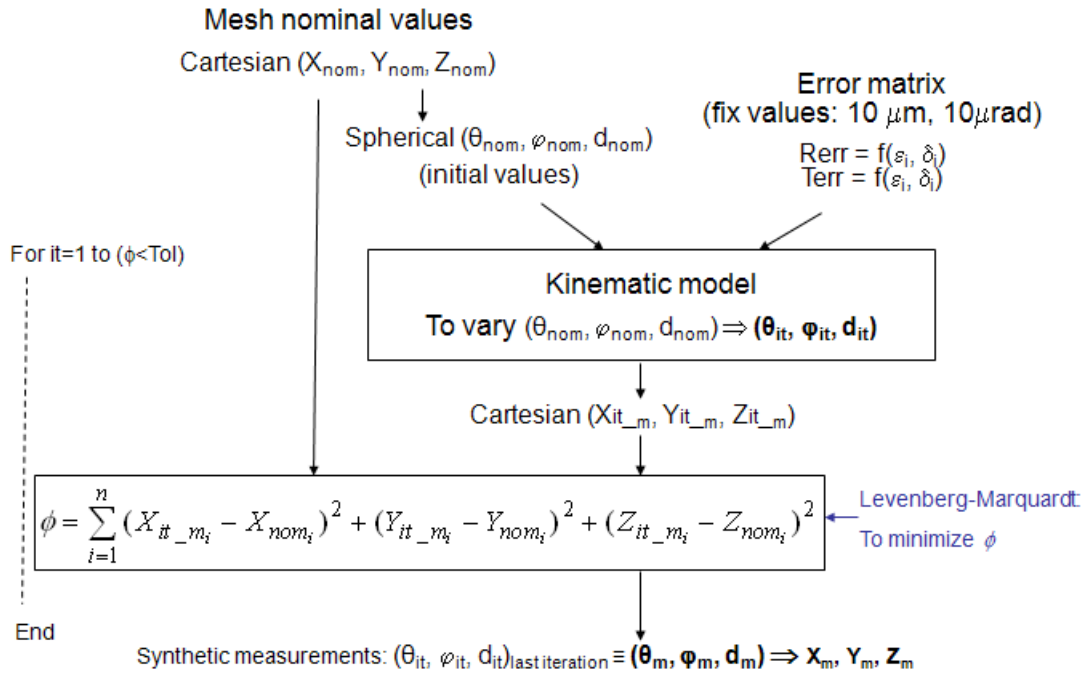

Fig. 6. Synthetic measurements by the kinematic model using mesh nominal values and error parameters.

4.2. Kinematic error parameter identification

The following step to validate the model is to correct synthetic measurements obtained in subsection 4.1. The output of the identification is the error parameter vector. This vector, $V\varepsilon$, is set to cero before starting the calibration, and will be modified in every iteration. In this case, nominal coordinates of the mesh of reflectors, (X_{nom}, Y_{nom}, Z_{nom}), and synthetic measurements, (X_m, Y_m, Z_m), are the known data. The kinematic model provides the Cartesian coordinates affected by the laser tracker error in the iteration *it*, (X_{it_m}, Y_{it_m}, Z_{it_m}), that minimize the objective function, shown by Equation 22 in every iteration. Figure 7 shows the procedure followed.

The calibration procedure allows us to identify the model error parameters. These parameters should have a value equal to the error parameters introduced in the kinematic model in the synthetic measurement generation given by Table 2. The values of the kinematic model parameters are the nominal values presented in Table 1.

Tables 3, 4 and 5, show the error parameters obtained in the parameter identification procedure for every mesh studied. To obtain a first approximation, errors defined by Equation 15 have been used, considering the first term of Equations from 16 to 21 in this simulation process and keeping the rest of parameters with a constant value of zero.

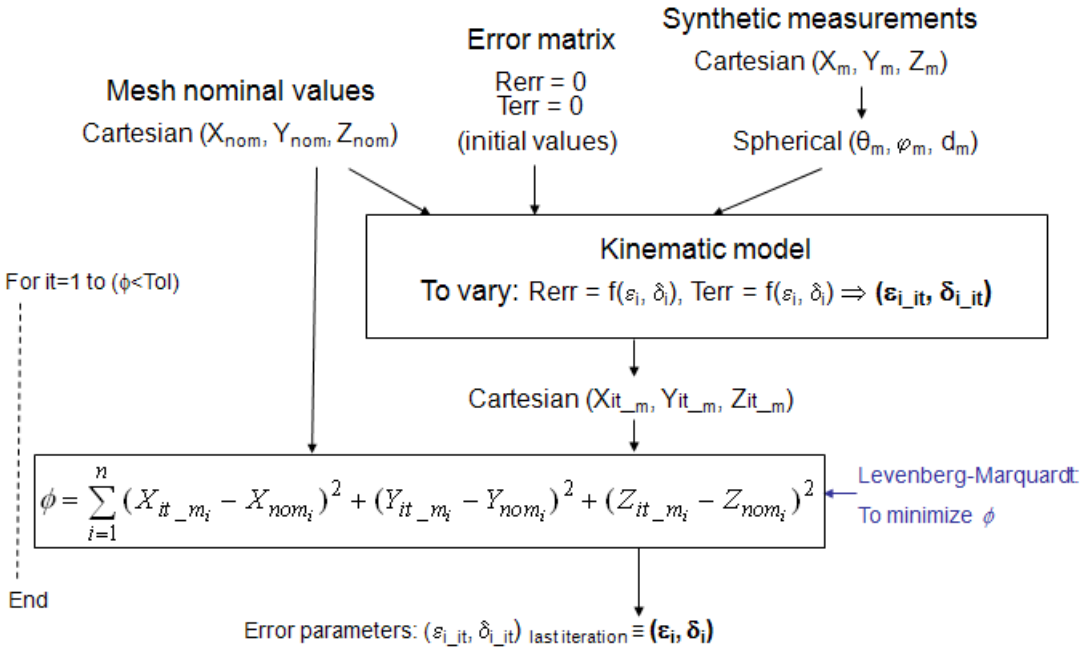

Fig. 7. Error parameters by the kinematic model using mesh nominal values and synthetic measurements.

Table 3. Error values obtained for a plane mesh in the parameter identification procedure.

	ε_X (μrad)	ε_Y (μrad)	ε_Z (μrad)	δ_X (μm)	δ_Y (μm)	δ_Z (μm)
θ	9.992	9.992	-15.727	-12.359	-13.593	0.000
φ	9.976	40.307	53.778	10.136	1.340	8.150
d	9.912	-33.814	0.000	10.033	11.619	9.947

Table 4. Error values obtained for a cubic mesh in the parameter identification procedure.

	ε_X (μrad)	ε_Y (μrad)	ε_Z (μrad)	δ_X (μm)	δ_Y (μm)	δ_Z (μm)
θ	9.997	10.001	-1.178	9.997	9.997	-0.024
φ	9.998	-1.176	9.999	9.999	-0.037	-0.358
d	0.000	0.000	0.000	-0.373	10.005	10.003

Table 5. Error values obtained for a spherical mesh in the parameter identification procedure.

	ε_X (μrad)	ε_Y (μrad)	ε_Z (μrad)	δ_X (μm)	δ_Y (μm)	δ_Z (μm)
θ	9.994	9.994	-5.101	10.001	9.977	0.000
φ	9.986	-5.137	9.416	10.045	0.000	9.969
d	9.966	10.574	0.000	10.011	9.969	10.018

Most of the error parameters obtained are very similar to the initial parameters and some of them differ because different parameters can generate very similar errors by themselves or as combination of other parameters. Besides, the overall effect of some

parameters that are independent can be compensated in function of the captured points, that is to say, in function of the position that presents the LT axes in data acquisition process.

Figure 8 shows the distances between nominal and measured positions, as obtained before by Equation 22. Sub-index *ini* represents initial values and sub-index *res* corresponds to residual values.

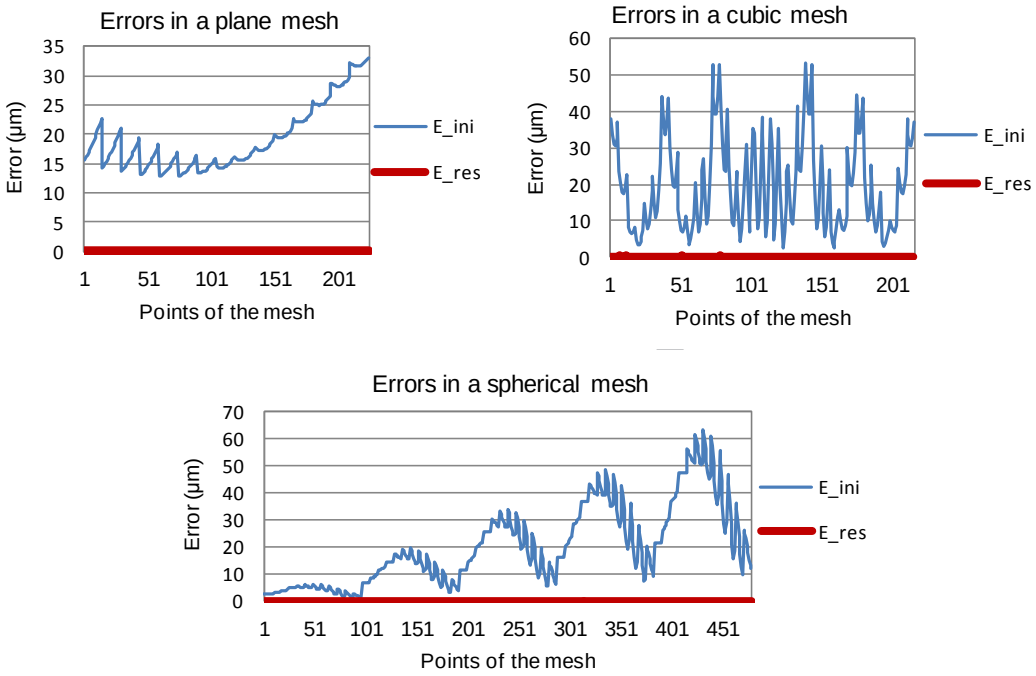

Fig. 8. Identification procedure: initial and residual error.

The residual error is very close to zero, as it was expected. This fact validates the developed model.

The plane mesh presents lower errors than cubic and spherical mesh, and the magnitude order is the same in all the mesh studied.

5. Experimental parameter identification

5.1. Data acquisition

Once the kinematic model has been validated by means of synthetic data, the same process is carried out using experimental data measured by the LT.

The first step is data acquisition. To do this, 17 reflectors were located on a CMM, with an accuracy of ± 2 µm, as shown in Figure 9a. The LT was located in 5 positions (see Figure 9b).

The reflectors were measured with the CMM. These measurements are considered the nominal measurements in the data acquisition step.

The LT then measured every reflector in every position, as shown in Figure 10, thus obtaining data measurements.

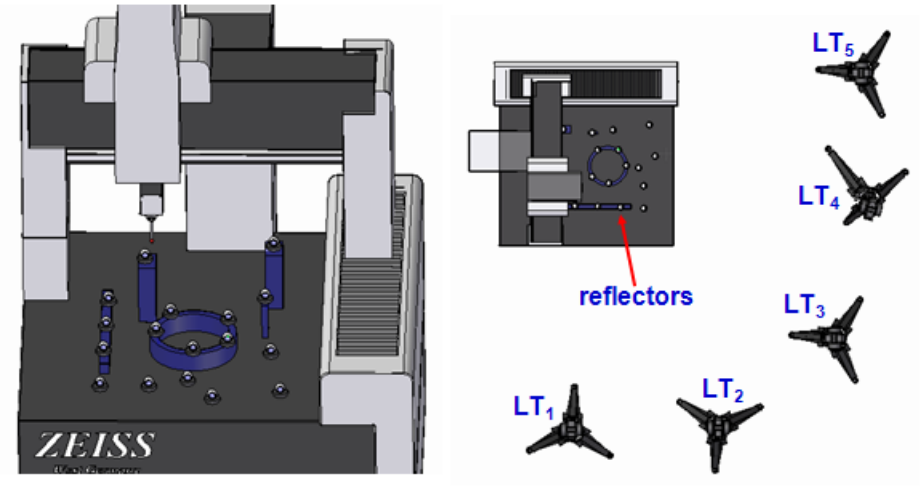

(a) (b)

Fig. 9. Data acquisition procedure: a) Reflector positions located on a CMM, b) LT positions.

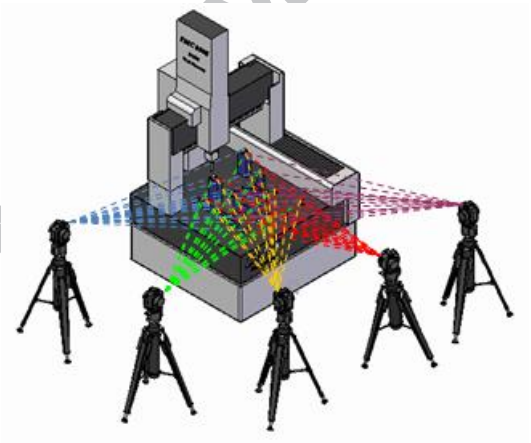

Fig. 10. LT measurements.

5.2. Identification procedure

The aim of this process is to search for the values of the error parameters that minimize the measurement error. However, in this case, measurements are experimental. Figure 11 shows the procedure described. Reflector nominal coordinates are measured by the CMM, thus obtaining (X_{nom}, Y_{nom}, Z_{nom}). The reflector Cartesian coordinates, (X_m, Y_m, Z_m), are then measured by the LT and transformed to Spherical coordinates (θ_m, φ_m, d_m). The output of the kinematic model is the Cartesian coordinates that would measure the LT for the value of the parameters (ε_i, δ_i) in the iteration *it*, (X_{it_m}, Y_{it_m}, Z_{it_m}). The objective function minimizes the differences between all nominal distances given by

every pair of reflectors (measured by the CMM), d_{CMMi}, and the same distances measured by every LT, d_{mik}, for k LT positions.

17 reflectors were used to cover in a regular way the CMM workspace. After analysing the possible capture angle for these reflectors, placed in fix positions, 5 LT positions were needed to cover it.

The number of distances is a combination without repetition of n elements taken r at a time, as shown by Equation 23.

$$C_{n,r} = \frac{n!}{r!(n-r)!} \tag{23}$$

The number of distances calculated for every position of the LT having 17 reflectors is 136. Thus, the number of distances to optimize for the 5 positions is 680 distances.

Equation 24 gives the objective function.

$$\phi = \sum_{i=1}^{C_{n,r}} \sum_{k=1}^{LT} (d_{m_{ik}} - d_{CMM_i}) \tag{24}$$

where sub-index m is the measured distance obtained from the measurements of the LT, sub-index CMM is the measured distance obtained from the measurements of the CMM, sub-index i defines the distance to minimize, and k corresponds to the position of the LT.

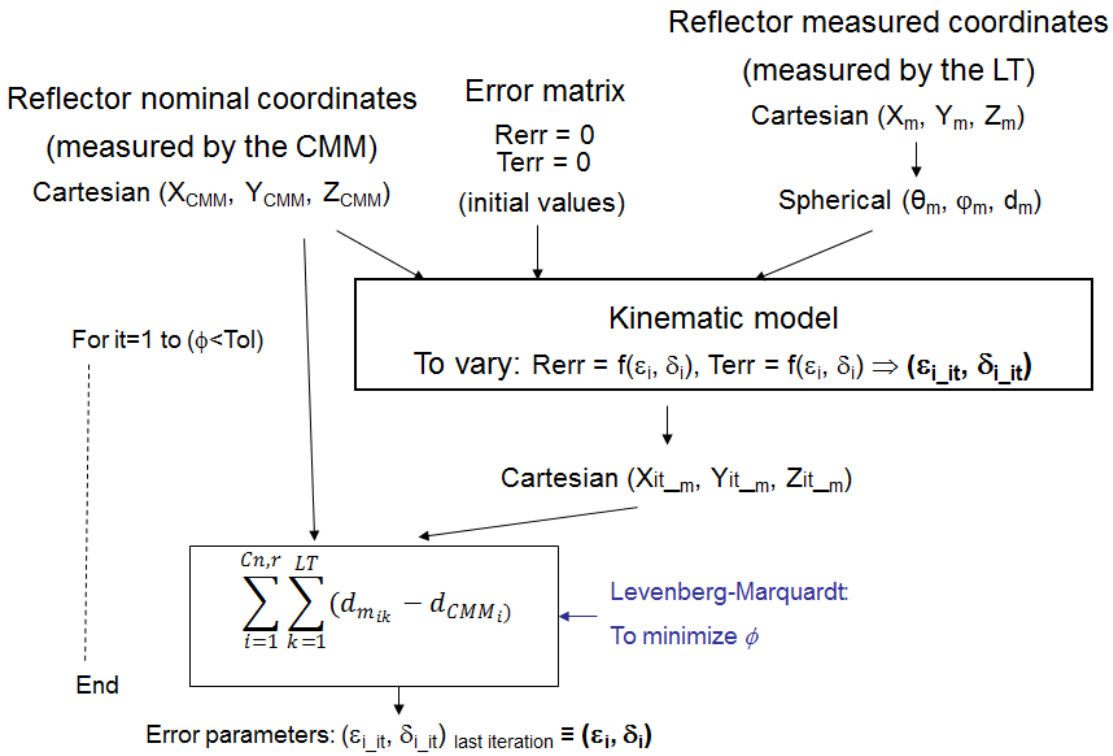

Fig. 11. Error parameters by the kinematic model using the reflector nominal coordinates measured by the CMM and the reflector coordinates measured by the LT.

The kinematic parameter identification is usually carried out by means of approximation procedures based on least-squares fitting. The optimization technique used to solve the numerical optimization algorithm was the Levenberg-Marquart (L-M) [27] method, due to its proven efficiency in non-linear systems [33].

As it was mentioned in the data acquisition step, 17 reflectors were measured locating the LT in 5 positions. To perform the optimization, different strategies have been carried out:

a) The optimization is performed using the 17 reflectors and the 5 LTs.
b) The optimization is performed using 14 reflectors and the 5 LTs. 3 reflectors are kept as test data. Thus, the model will be validated in positions different from those used in the identification process.
c) The optimization is performed using 17 reflectors and 4 LT positions. 1 LT position is kept as verification data.

The results obtained in every strategy followed are presented below.

Figure 12 illustrates the LT position error calculated as the difference between the error before the identification procedure, *E_ini*, and the error after performing the kinematic parameter identification for the three strategies a), b) and c). Strategy a) provides the error *E_res*. The error obtained is given by *E_4LT* when the positions measured by 4 LT are used in the identification procedure and 1 LT measurements are kept as test positions for the parameter evaluation procedure. Finally, *E_14_ref* corresponds to the error when the measurements of 14 reflectors are used in the identification procedure and the measurements of 3 reflectors are kept as test positions. 5 LT measurements are represented consecutively. The optimization that provides *E_res* was performed considering all measured points in the parameter identification. The points measured by L_1 were kept as test positions in the parameter identification that gives *E_4LT*. Finally, the first thirty-five positions of each LT were kept as test positions in the parameter identification that provides *E_14_ref*.

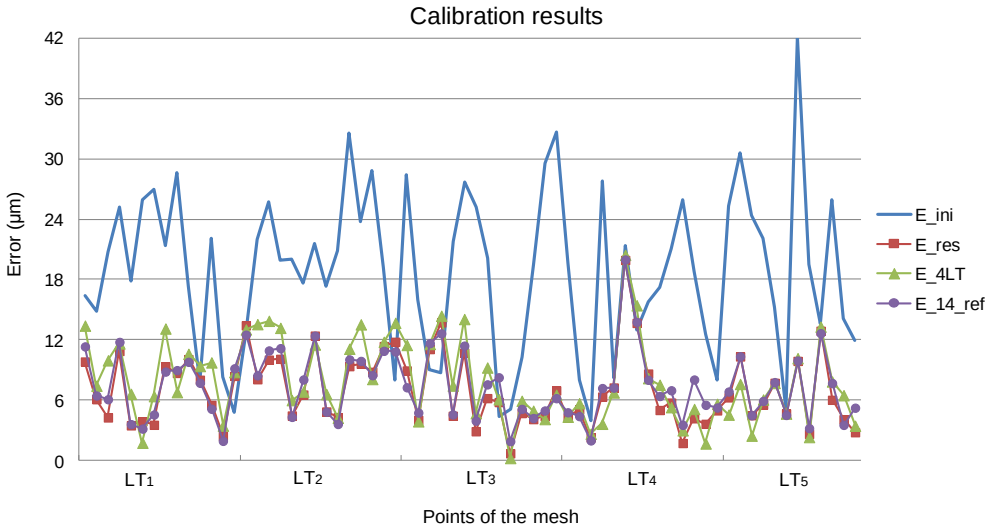

Fig. 12. Calibration results.

Table 6 shows the maximum and mean errors obtained considering all points, the calibration points and the test points for every strategy.

The correction performed by means of the identification procedure decreases errors about a 62.50% using the strategy a), about a 57.47% using the strategy b) and 60.44% using the strategy c) with respect to initial errors. As it was expected, strategy a) presents the lower errors because all data have been included into the optimization. The difference between strategy a) and strategies b) and c) has a mean value of 1.54 μm and 0.74 μm for strategies b) and c), respectively, and a maximum value of 5.67 μm and 3.85 μm for strategies b) and c), respectively. These results verify that the identification procedure developed can be extrapolated to different positions within the LT workspace from those used in the identification procedure. Moreover, calibration results improve when some reflectors are kept as test positions with respect to decrease LT positions.

Table 6. LT initial errors and LT errors for every strategy.

	E_ini (μm)	E_res (μm)	E_4LT (μm)			E_14_ref (μm)		
			All points	Calibration points	Test points	All points	Calibration points	Test points
Maximum	42.057	19.935	20.446	20.446	14.394	19.981	19.981	11.342
Mean	18.785	7.045	7.989	7.391	9.973	7.430	7.490	7.152

Figure 13 represents results after calibration to compare the strategies followed.

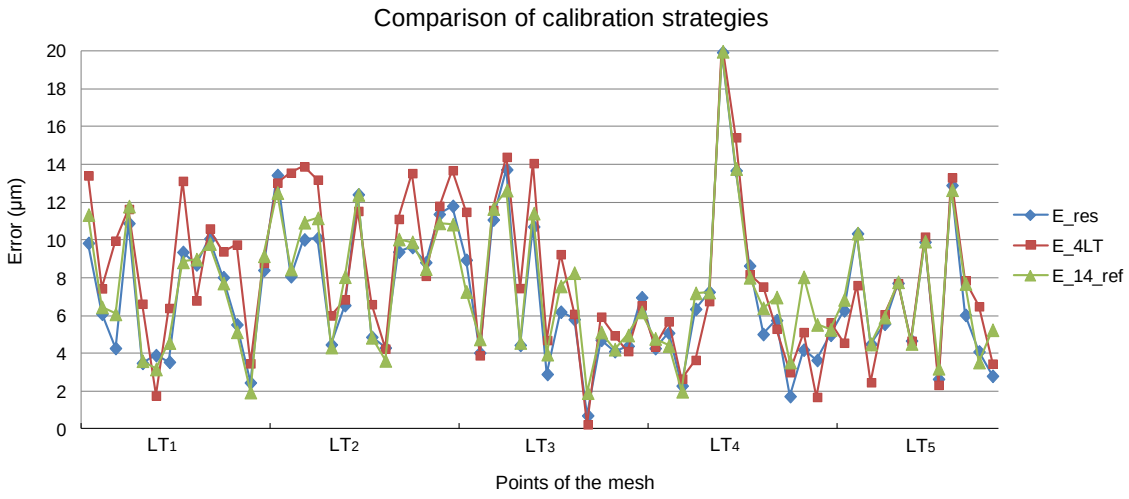

Fig. 13. Comparison of calibration strategies.

6. Sensitivity analysis of the length measurement system tests

Once the kinematic model developed has been validated, the following step will be to perform a sensitivity analysis of the length measurement system tests.

The objectives of the sensitivity analysis are the following:

- To help us to design measurement tests sensitive to error parameters, thus, defining the most suitable target position configuration to carry out the calibration procedure. This analysis obtains how every individual error affects the total error, showing how model errors affect the LT measurement.
- To know the best possible positions to carry out experimental tests, thus, designing the configuration of network with fix points. This analysis obtains how reflector positions of tests affect in the error.

The spherical mesh, shown in Figure 5c, is the mesh chosen for the sensitivity analysis because this mesh allows us to find out the correlation between parameters θ, φ and d and the errors more clearly as it fits the LT working range.

This analysis has been performed by studying the 18 error parameters from the kinematic model developed in subsection 3.1, -corresponding to the error matrices. To analyse the influence of every error considered in the global error, 18 simulations were carried out, setting up a value of 1 for every parameter and zero for the rest of parameters. Sensitivity represents the error in micrometers for 1 μm of offset for linear errors and 1 μrad of tilt for rotational errors.

The measurement error has been studied in every simulation in function of vertical angle (V), horizontal angle (H) and distances (R).

Figure 14 represents the results obtained for every error parameter studied. This figure shows first, vertical angle variations between 77º and -60º, second, horizontal angle variations from 1º to 360º with increments of 12º, and finally, distance variations between 1 m and 15 m with increments of 3.5 m. Divisions in X axis represent the measurement number. 480 measurements were performed, and every measurement presents different values of R, H and V.

The results obtained shows that the error parameter ε_{ZR}, corresponding to a rotation of the laser beam with respect to an axis in the beam direction, does not affect. There are 12 errors, δ_{XH}, δ_{YH}, δ_{ZH}, ε_{ZV}, δ_{XV}, δ_{YV}, δ_{ZV}, ε_{XR}, ε_{YR}, δ_{XR}, δ_{YR}, δ_{ZR}, present a constant error proportional to the error parameter. And there are 5 errors that depend on both the distance of the LT to the reflectors and the azimuth and elevation angles. The simulation has been carried out considering 5 areas. As can be seen, in area 1 (corresponding to distance *R=1 m)*, the last 5 parameters vary from 0 to 1 μm, in area 2, (corresponding to distance *R=4.5 m)*, the last 5 parameters vary from 0 to 4.5 μm, etc. This findings verify that the 5 parameter values vary from 0 to R $\mu m/m$. To study the behaviour of these 5 parameters, the number of points has been increased, with increments of 9.78º for vertical angles and of 12º for horizontal angles. Figure 15 represents only half period ($\pi/2$) because the error presents a cyclic behaviour, with a cycle π, in the azimuth angle.

This analysis shows that the positions presenting high sensitivity to error parameters are those that correspond to elevation angles with minimum (-60º), zero value (0º) and maximum (77º). Moreover, the errors caused by rotary errors in *X* and *Y* of the horizontal angle are also sensitive to this same rotation. Tests should be configured setting up directions in which points are more sensitive to errors.

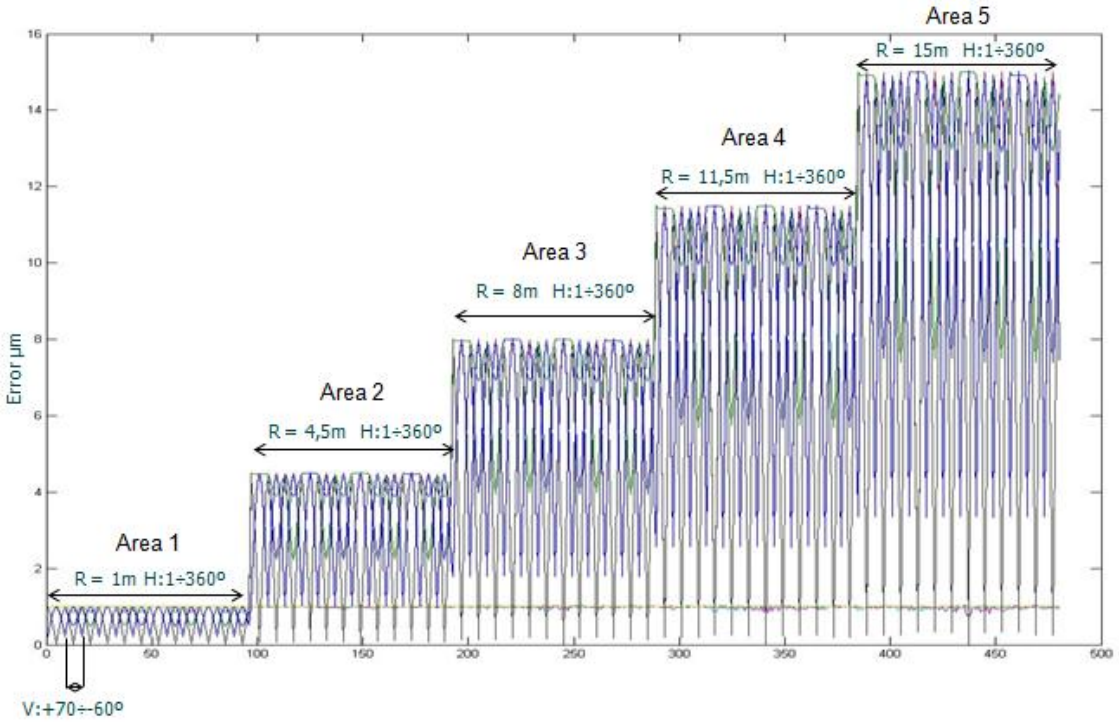

Fig. 14. Sensitivity analysis of the length measurement system tests. H≡θ, V≡φ, R≡d.

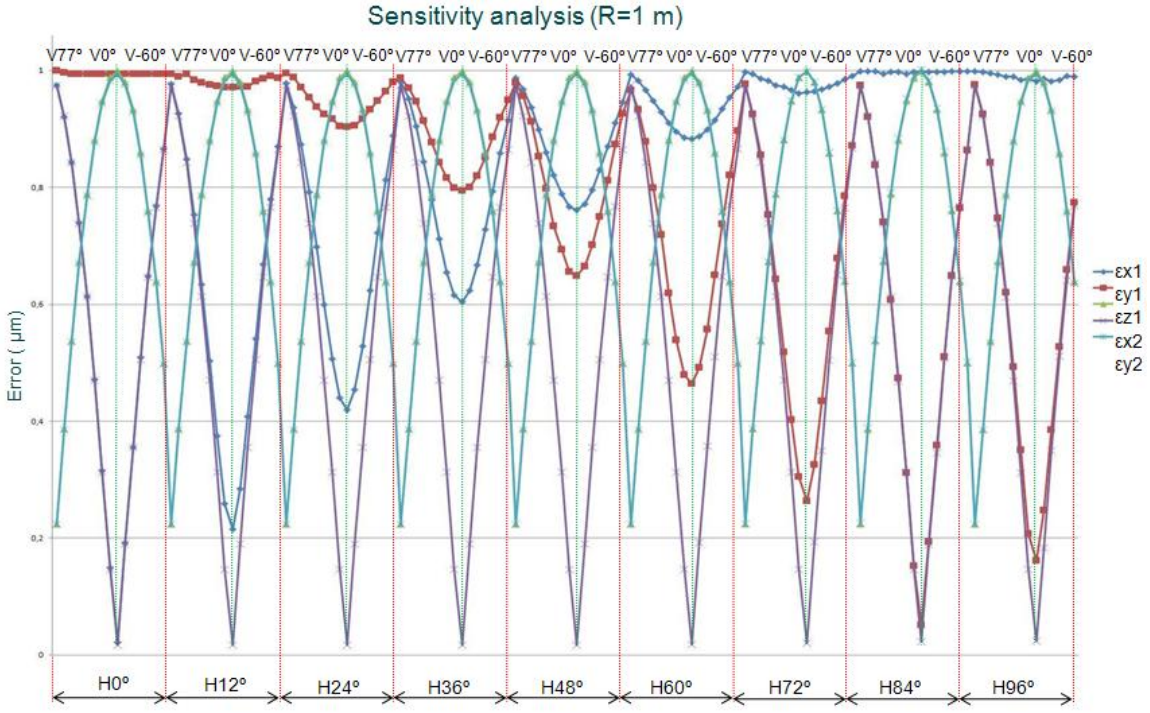

Fig. 15. Errors presenting dependence on θ and φ for a constant distance of 1 m.

7. Conclusions.

A LT user can know the LT behaviour after calibrating the LT. However, he cannot know if the LT works properly after a while or if a calibration should be carried out. Moreover, the tests recommended by standards to validate the LT behaviour require specialized equipment and take a lot of time.

A new kinematic model for a LT having the beam source in the rotating head has been developed. This model considers that errors depend on joints. The kinematic model behaviour has been validated, generating synthetic measurements for a known nominal reflector coordinates and error parameters, thus, obtaining the values that would measure the LT if it had the prefixed errors. Measurements have then been corrected by identifying error parameters, thus, obtaining error parameters by means of the kinematic model. The comparison of the prefixed initial error parameters and the error values obtained allows us to validate the kinematic model developed.

All these verifications have been made for different meshes, obtaining that the spherical mesh is the one that allows us to analyse the correlation between parameters θ, φ and d and the errors more clearly.

An experimental calibration has then been performed, measuring the reflectors with both a CMM that provides nominal values and a LT located in different positions. To do this, different strategies have been followed, keeping different measurements as test positions. The parameter identification performed allows us to reduce the LT error about a 62%. Results show that the different strategies analyzed provide a calibration that can be extrapolated to different positions from those used in the identification procedure within the LT workspace. Moreover, calibration results improve when some reflectors are kept as test positions with respect to decrease LT positions.

Finally, a sensitivity analysis of the length measurement system tests has been performed. This analysis shows the dependence on elevation and azimuth angles and on distances of every error parameter. Moreover, the analysis indicates those positions with more sensitivity, given by maximum, minimum and zero vertical angle, setting up the bases for the most suitable test configurations for the calibration procedure.

The LT verification method developed allows us to know in an easy and fast way if the LT measures correctly, obtaining the LT errors without requiring standards and accurate equipment.

8. References

1. Wang Z, Mastrogiacomo L, Franceschini F, Maropoulos P (2011) Experimental comparison of dynamic tracking performance of iGPS and laser tracker. Int J Adv Manuf Technol 56:205-213

2. Burge JH, Su P, Zhao C, Zobrist T (2007) Use of a commercial laser tracker for optical alignment:66760E-66760E-12

3. Huo D, Maropoulos PG, Cheng CH (2010) The Framework of the Virtual Laser Tracker–A Systematic Approach to the Assessment of Error sources and Uncertainty in Laser Tracker Measurement:507-523

4. Nubiola A, Bonev IA (2012) Absolute calibration of an ABB IRB 1600 robot using a laser tracker. Robot Comput Integrated Manuf

5. Aguado S, Samper D, Santolaria J, Aguilar JJ (2012) Identification strategy of error parameter in volumetric error compensation of machine tool based on laser tracker measurements. Int J Mach Tools Manuf 53:160-169

6. Koseki Y, Arai T, Sugimoto K, Takatuji T, Goto M (16-20 May 1998) Design and accuracy evaluation of high-speed and high precision parallel mechanism 3:1340-1345

7. Meng G, Tiemin L, Wensheng Y (5-8 October 2003) Calibration method and experiment of Stewart platform using a laser tracker 3:2797-2802

8. Santolaria J, Majarena AC, Samper D, Brau A, Velázquez J (2014) Articulated Arm Coordinate Measuring Machine Calibration by Laser Tracker Multilateration. The Scientific World Journal 2014:681853-1-681853-11

9. Yan B, Wang J, Lu N, Deng W, Dong M, Lou X (2008) Application of laser tracker used in the measuring and the adjusting of the workbench for SAR antenna:71552M-71552M-8

10. Zobrist TL, Burge JH, Davison WB, Martin HM (2008) Measurements of large optical surfaces with a laser tracker:70183U-70183U-12

11. Barazzetti L, Giussani A, Roncoroni F, Previtali M (2013) Monitoring structure movement with laser tracking technology:879106-879106-12

12. Sładek J, Ostrowska K, Kohut P, Holak K, Gąska A, Uhl T (2012) Development of a vision based deflection measurement system and its accuracy assessment. Measurement

13. Umetsu K, Furutnani R, Osawa S, Takatsuji T, Kurosawa T (2005) Geometric calibration of a coordinate measuring machine using a laser tracking system. Measurement Science and Technology 16:2466

14. Muralikrishnan B, Lee V, Blackburn C, Sawyer D, Phillips S, Ren W, Hughes B (2013) Assessing ranging errors as a function of azimuth in laser trackers and tracers. Measurement Science and Technology 24:065201

15. Muralikrishnan B, Sawyer D, Blackburn C, Phillips S, Borchardt B, Estler W (2009) ASME B89. 4.19 performance evaluation tests and geometric misalignments in laser trackers. Journal of Research of the National Institute of Standards and Technology 114:21-35

16. ASME B89.4.19-2006 Standard . Performance Evaluation of Laser-Based Spherical Coordinate Measurement Systems www.asme.org

17. Majarena AC, Santolaria J, Samper D, Aguilar JJ (2011) Modelling and calibration of parallel mechanisms using linear optical sensors and a coordinate measuring machine. Measurement Science and Technology 22:105101-1-12

18. Denavit J, Hartenberg RS (1955) A kinematic notation for lower-pair mechanisms based on matrices. Trans. ASME J. Appl. Mech 22:215-221

19. Chiang MH, Lin HT, Hou CL (2011) Development of a stereo vision measurement system for a 3D three-axial pneumatic parallel mechanism robot arm. Sensors 11:2257-2281

20. Gatti G, Danieli G (2008) A practical approach to compensate for geometric errors in measuring arms: application to a six-degree-of-freedom kinematic structure. Measurement Science and Technology 19:015107

21. Pereira P, Di Giacomo B (2008) Thermal error evaluation and modelling of a CNC cylindrical grinding machine. Metrologia 45:217

22. Du G, Zhang P (2013) IMU-based online kinematic calibration of robot manipulator. The Scientific World Journal 2013

23. Hsu TW, Everett LJ (August 1985) Identification of the kinematic parameters of a robot manipulator for positional accuracy improvement:263-267

24. Everett LJ, Suryohadiprojo AH (24-29 April 1988) A study of kinematic models for forward calibration of manipulators 2:798-800

25. He J, Gao F, Bai Y (2013) A two-step calibration methodology of multi-actuated mechanical servo press with parallel topology. Measurement 46:2269-2277

26. Majarena A, Santolaria J, Samper D, Aguilar J (2013) Analysis and evaluation of objective functions in kinematic calibration of parallel mechanisms. The International Journal of Advanced Manufacturing Technology:1-11

27. Levenberg K (1944) A method for the solution of certain non-linear problems in least squares. Quart.Appl.Math 2:164–168

28. Gassner G, Ruland R (2008) . Laser Tracker Calibration-Testing the Angle Measurement System

29. Ouyang J, Liu W, Qu X, Yan Y, Liang Z (2007) Modeling and self-calibration of laser tracker system using planar constraints

30. Zhuang H, Motaghedi SH, Roth ZS, Bai Y (2003) Calibration of multi-beam laser tracking systems. Robot Comput Integrated Manuf 19:301-314

31. Takatsuji T, Goto M, Kirita A, Kurosawa T, Tanimura Y (2000) The relationship between the measurement error and the arrangement of laser trackers in laser trilateration. Measurement science and technology 11:477

32. Slocum AH (1992) Precision machine design. Prentice Hall, Englewood Cliffs, New Jersey

33. Gao Z, Zhang D, Ge Y (2010) Design optimization of a spatial six degree-of-freedom parallel manipulator based on artificial intelligence approaches. Robot Comput Integrated Manuf 26:180-189

HIGHLIGHTS

- Development of a kinematic model of a Laser Tracker
- Development of a synthetic generator to validate the kinematic model
- Calibration of a Laser Tracker to improve the system accuracy
- Sensitivity analysis of the length measurement system tests
- More suitable positions to perform the calibration procedure